Available online at www.sciencedirect.com
ScienceDirect
Spectrochimica Acta Part A 67 (2007) 1392–1397
SPECTROCHIMICA ACTA PART A
www.elsevier.com/locate/saa

Phosphorus–nitrogen compounds: Synthesis and spectral investigations on new *spiro*-cyclic phosphazene derivatives

Hakan Dal *, Yasemin Süzen

Department of Chemistry, Faculty of Science, Anadolu University, 26470 Yenibağlar, Eskişehir, Turkey

Received 27 May 2006; received in revised form 7 October 2006; accepted 18 October 2006

Abstract

The condensation reaction of {*N*-[(2-hydroxyphenylmethyl)amino]-4,6-dimethylpyridine} (**2**), which is a reduction product of **1**, with trimer $N_3P_3Cl_6$ affords partially a substituted *spiro*-cyclic phosphazene derivative (**3**). The fully substituted phosphazenes (**4** and **5**) have also been obtained from the reactions of **3** with the excess of pyrrolidine and morpholine. The characterizations and spectral investigations of these compounds have been made by elemental analyses, FTIR, ^{1}H-, ^{13}C-, ^{31}P NMR, correlation spectroscopy (COSY), heteronuclear chemical shift correlation (HETCOR), heteronuclear multiple-bond correlation (HMBC) and mass spectroscopy (MS). The salient features of spectral data of these compounds have been discussed.

Keywords: Synthesis of phosphazene derivatives; *spiro*-Phosphazenes; Spectroscopic studies of phosphazenes; HETCOR; HMBC

1. Introduction

Cyclophosphazenes are an important family of inorganic ring systems, which traditionally have received attention for two main reasons: (i) to obtain small molecules of phosphazene derivatives [1,2] and (ii) to produce polymeric phosphazene derivatives [3]. They also play an important role in the chemistry of heteroatom compounds. In recent years, phosphazene polymers have attracted considerable attention because they can be tailored to possess a wide variety of physical and chemical properties by changing the side groups [4,5]. The coordination chemistry of the various multi-site ligands derived from cyclophosphazenes is extremely interesting new area. Phosphazenes have been proposed for a broader array of applications including flame-retardants [6,7], rechargeable lithium batteries [8,9], microencapsulant membranes, high performance fluids and ionic conductors [10], the further design of the highly selective anticancer [11], antibacterial [12], anti-HIV [13] and artificial bone [14] agents.

In this study, the novel *spiro*-cyclic phosphazene derivatives (**4**,**5**) have been obtained (Scheme 1) and their spectroscopic characterizations have been carried out. Total assignments of ^{1}H-, ^{13}C- and ^{31}P NMR spectra for the structures were made with help of H–H correlation spectroscopy (H–H COSY), as well as heteronuclear chemical shift correlation (HETCOR) and heteronuclear multiple-bond correlation (HMBC).

2. Experimental

2.1. Reagents and materials

Hexachlorocyclotriphosphazatriene, $N_3P_3Cl_6$, was purchased from Aldrich and recrystallized from dry hexane followed by sublimation twice before use. 2-Hydroxybenzaldehyde, triethylamine (99.5%), aminopyridines and sodium borohydride were purchased from Fluka and used as received. All experimental manipulations were carried out under argon atmosphere. Solvents tetrahydrofuran (98%), dichloromethane (98%), acetonitrile (99.5%) and light petroleum were dried by standard methods prior to use. Melting points were measured on a Gallenkamp apparatus using a capillary tube. ^{1}H-, ^{13}C-, ^{31}P NMR, HETCOR and HMBC spectra were obtained on a Bruker DPX FT NMR (500 MHz) spectrometer ($SiMe_4$ as internal standard and 85% H_3PO_4 as an external standard). Spectrometer equipped with a 5 mm PABBO BB-inverse gradient probe. The concentration of solute molecules was 150 mg in 1.0 mL $CDCl_3$. Standard Bruker pulse

* Corresponding author. Tel.: +90 222 335 05 80; fax: +90 222 320 49 10.
E-mail address: hakandal@anadolu.edu.tr (H. Dal).

1386-1425/$ – see front matter © 2006 Elsevier B.V. All rights reserved.
doi:10.1016/j.saa.2006.10.029

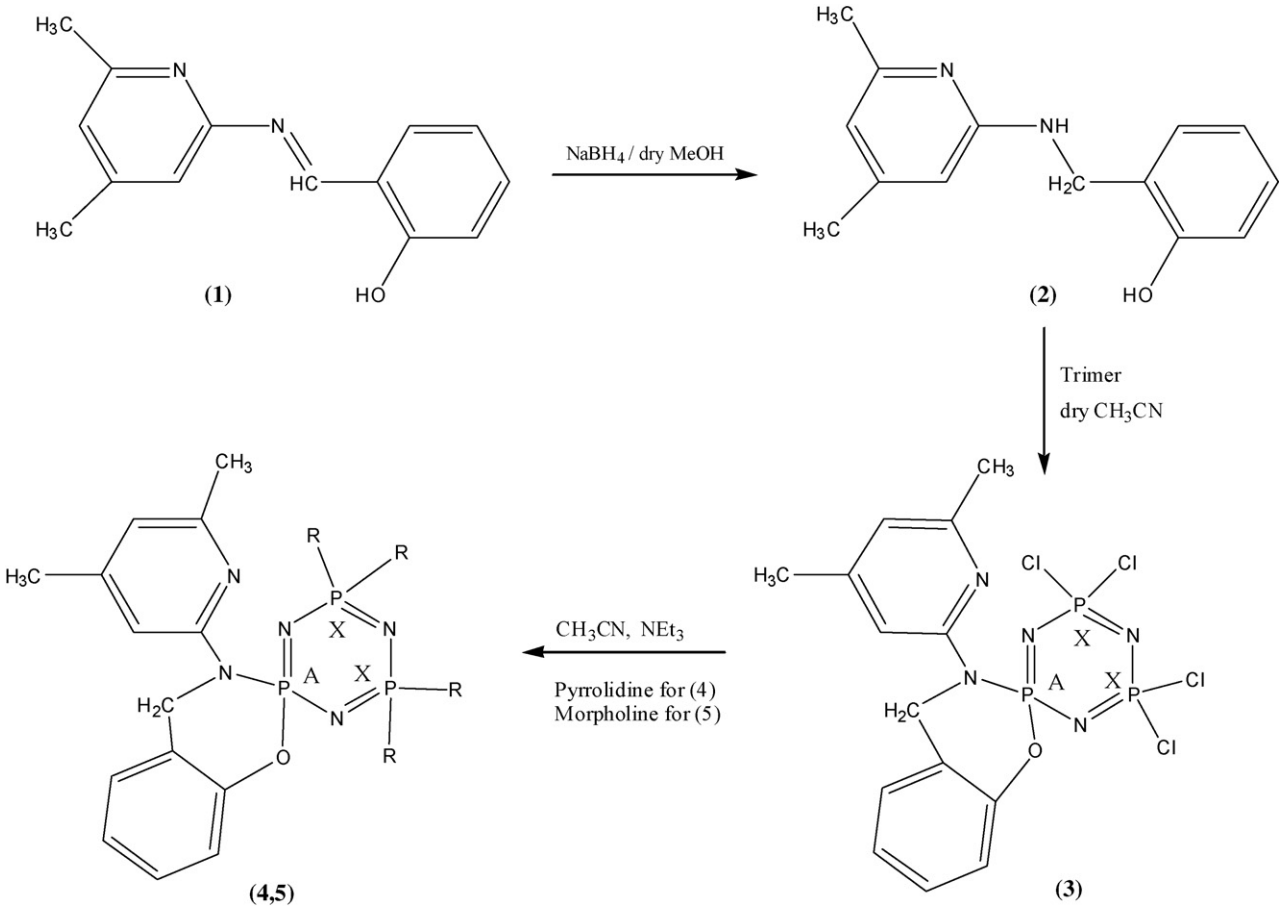

Scheme 1.

programs [15] were used throughout the entire experiment. FTIR spectra were recorded on a Jasco 300E FTIR spectrometer in KBr discs and were reported in cm^{-1} units. Microanalyses were carried out by Medicinal Plants and Medicine Research Center of Anadolu University Eskişehir (Turkey). Electrospray ionization mass spectrometric (ESI-MS) analyses were performed on the AGILEND 1100 MSD spectrometer.

2.2. Synthesis of ligands

Preparation of compounds (**1**–**3**) were carried out as in Scheme 1, adapting a reported procedure [16]. 2-[(1E)-2-aza-2-(4,6-dimethyl(2-pyridyl))vinyl] (**1**) has been obtained using a method in which salicylaldehyde (4.87 g, 3.99 mmol) and 4,6-dimethyl-2-aminopyridines (4.88 g, 3.99 mmol) were refluxed in MeOH (50 mL). The resulting solid was crystallized from MeOH. For the synthesis of *N*-[2-hydroxy(phenylmethyl)amino]-4,6-dimethylpyridine (**2**), 2-[(1E)-2-aza-2-(4,6-dimethyl(2-pyridyl))vinyl] (**1**) (7.64 g, 33.9 mmol) was refluxed in MeOH (50 mL) for 1 h and then equimolar amount of sodium borohydride (1.28 g, 33.9 mmol) was partially added to the reaction mixture. The reduction was completed after 2 h. Then, the solvent was evaporated in reduced pressure, the residue was dissolved in dichloromethane and washed with water. Compound (**2**) was crystallized from MeOH.

2.3. Synthesis of phosphazene derivatives

4,4′,6,6′-Tetrachloro-3,4-dihydro-3-(4,6-dimethylpyridin-2-yl)*spiro*-[1,3,2-benzoxazaphosphinine-2,2′-(2λ^5,4λ^5,6λ^5-cyclotriphosphazene)] (**3**), the synthesis and solid state structure of **3** have been published and it was prepared according to the published procedure [17]. 4,4′,6,6′-Tetrapyrrolidine-3,4-dihydro-3-(4,6-dimethylpyridin-2-yl)*spiro*-[1,3,2-benzoxazaphosphinine-2,2′-(2λ^5,4λ^5,6λ^5-cyclotriphosphazene)] (**4**), 4,4′,6,6′-tetrachloro-3,4-dihydro-3-(4,6-dimethylpyridin-2-yl)*spiro*-[1,3,2-benzoxazaphosphinine-2,2′-(2λ^5, 4λ^5, 6λ^5-cyclotriphosphazene)] (**3**) (2.17 g, 3.38 mmol) and pyrrolidine (1.92 g, 2.24 mL, 27.04 mmol) in acetonitrile (150 mL) were allowed to react by refluxing 62 h. After work-up it was done as in synthesis of compound **3** crystallized from THF/*n*-hexane (2:1), $R_f = 0.57$ [*n*-hexane/THF (2:1)]. 4,4′,6,6′-Tetramorpholine-3,4-dihydro-3-(4,6-dimethylpyridin-2-yl)*spiro*-[1,3,2-benzoxazaphosphinine-2,2′-(2λ^5,4λ^5,6λ^5-cyclotriphosphazene)] (**5**), the work-up procedure of this compound was as in the preparation of **4**. It was recrystallized from THF/light petroleum (bp 40–60) (2:1) $R_f = 0.76$ [THF/*n*-hexane (2:1)]. Experimental and analytical data are listed in Table 1. The ESI-MS spectra of compounds (**1**, **3**–**5**) show the protonated $[M+H]^+$ and deprotonated $[M-H]^+$molecular ion peaks. The elemental analyses results are in agreement with the proposed structures.

Table 1
Experimental and analytical data

Compound	Empirical formula	MW	Yield (%)	mp (°C)	Calculated (found) (%) C	H	N
1	$C_{14}H_{14}N_2O$	226.27	85	94	74.31 (73.89)	6.24 (5.32)	12.38 (13.51)
2	$C_{14}H_{16}N_2O$	228.29	90	109	73.66 (73.42)	7.06 (6.41)	12.27 (13.05)
3	$C_{14}H_{14}Cl_4N_5OP_3$	500.92	72	228	33.43 (34.32)	2.81 (2.67)	13.92 (13.83)
4	$C_{30}H_{46}N_9OP_3$	641.30	59	153	56.15 (56.54)	7.23 (7.10)	19.65 (19.41)
5	$C_{30}H_{46}N_9O_5P_3$	705.67	51	234	51.06 (51.62)	6.57 (6.26)	17.86 (18.51)

Table 2
Selected IR bands

Compound	$\nu_{(N–H)}$	$\nu_{(C–H)\ arom}$	$\nu_{(C–H)\ alip}$	$\nu_{(C=C)}$	$\nu_{(P=N)}$	$\nu_{(P–Cl)}$
1	–	3061 m	2918 m	1544 vs	–	–
2	3421 vs	3049 m	2958; 2924 m	1587 s	–	–
3	–	3089 m	2950; 2853 m	1577 s	1189; 1228 vs	516; 578 s
4	–	3093 m	2962; 2860 s	1560 s	1170; 1225 vs	–
5	–	3087 m	2964; 2962 vs	1570	1188; 1256 vs	–

Abbreviations: s, strong; m, medium; v, very.

3. Results and discussion

Table 1 lists the empirical formulae, yields, molecular weights, melting points and partial elemental analyses for the compounds (**1**–**5**). Selected FTIR frequencies of various diagnostic bands of **1**–**5** are given in Table 2. In the FTIR spectra of the compounds characteristic $\nu_{N–H}$ and $\nu_{C–H}$ stretching bands are observed between 3421 cm^{-1} for **2** and 3093–3049 cm^{-1} for **1**–**5**. The absorption bands assignable to the stretching of the –P=N– for compounds (**3**–**5**) and P–Cl bands for **3** were ca. 1200 cm^{-1} and 516 and 578 cm^{-1}. These data are in accordance with the reported values for the similar phosphazene derivatives [16].

The proton decoupled (for **3**) and coupled for (**4** and **5**) ^{31}P NMR spectral data of *spiro*-phosphazenes are given in Table 3 and Fig. 1. ^{31}P NMR spectra show AX_2 spin system and they were critical for monitoring the degree to which the chlorine atoms in hexachlorocyclotriphosphazene had been substituted with bulky *spiro*-cyclo-*N*-methylpyridine groups. According to the pattern of proton coupled ^{31}P NMR spectra of **3**, it is concluded that the only *spiro*-architectures are possible. It is observed that $^2J_{(P,P)}$ values (48.6 and 49.9 Hz) of the fully substituted phosphazene derivatives (**4** and **5**) are smaller than the value (62.8 Hz) of *spiro*-phosphazene **3**. The $\delta(P_A)$ signal of **4** and **5** are downfield-shifted with respect to $\delta(P_A)$ of **3** by 6.79 and 5.58 ppm, respectively, while the signals of the tetrapyrrolidinyl-substituted and tetramorpholine-substituted P_X atoms of **4** and **5** are upfield-shifted with respect to corresponding P_X atom of **3** by 11.94 and 9.99 ppm, respectively, probably due to the lone electron pairs of the pyrrolidine or morpholine N-atoms of electron releasing to the P_X atoms. On the other hand, the chemical shifts are highly sensitive to the changes in the exocyclic NPN angles [18,19], thus the small variations in the angles possibly can deviate chemical shifts, significantly as observed in **3** (Table 3).

Proton magnetic resonance spectroscopy is a helpful tool for the identification of organic compounds in conjunction with other spectrometric informations. Table 4 lists complete ^1H- and ^{13}C NMR assignments for all of the compounds (**1**–**5**). The ^1H signals were assigned on the basis of chemical shifts, multiplicities and coupling constants. The two CH_3 protons of **3**–**5** are easily distinguishable, and they are observed at 2.68 and 2.46 ppm for **3**; 2.41 and 2.18 ppm for **4**; 2.42 and 2.90 ppm for **5** as singlets. In addition, in pyrrolidine and morpholine NCH_2 (Hg and Hg′) and NCH_2CH_2 (Hh and Hh′) protons of the rings

Table 3
$^{31}P(^1H)$ NMR spectral data in $CDCl_3$

Compound	δ (A)[a]	δ (X)[a]	$^2J_{PNP}$ (Hz)
3	6.43 (t)[b]	29.89 (d)	62.8
4	13.22 (tt)	17.95 (d)	48.6
5	12.01 (tt)	19.90 (d)	49.9

d: doublet, t: triplet.
[a] A and X are shown in Scheme 1.
[b] ^{31}P NMR spectrum is decoupled.

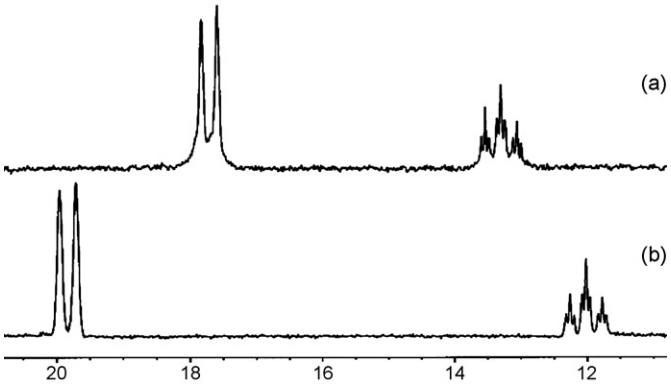

Fig. 1. $^{31}P(^1H)$ NMR spectrum in δ 11–30 ppm for: (a) compound **4** and (b) compound **5**.

Table 4
^{1}H- and ^{13}C NMR spectral data in $CDCl_3$

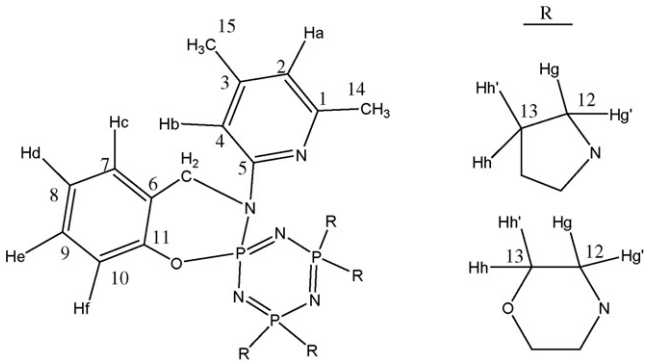

	Compounds				
	1	**2**	**3**	**4**	**5**
Ha	6.93 (s)	6.03 (s)	6.57 (s)	6.53 (s)	6.62 (s)
Hb	6.94–6.98 (m)	6.30 (s)	6.70 (s)	7.33 (s)	7.16 (s)
Hc	7.04 (d) [$^{3}J_{Hc–Hd}$ = 8.35]	6.98 (d) [$^{3}J_{Hc–Hd}$ = 8.03]	6.25 (m)	6.95 (d) [$^{3}J_{Hc–Hd}$ = 7.98]	6.96 (d) [$^{3}J_{Hc–Hd}$ = 8.23]
Hd	7.40 (t, d) [$^{3}J_{Hd–Hc,e}$ = 6.78] [$^{4}J_{Hd–Hf}$ = 1.69]	7.23 (t,d) [$^{3}J_{Hd–Hc,e}$ = 8.03] [$^{4}J_{Hd–Hf}$ = 1.66]	7.25 (m)	7.23 (m)	7.25 (m)
He	6.94–6.98 (m)	6.86 (t) [$^{3}J_{He–Hd,f}$ = 7.34]	7.20 (t) [$^{3}J_{He–Hd,f}$ = 7.53]	7.03 (t) [$^{3}J_{He–Hd,f}$ = 7.41]	7.07 (t) [$^{3}J_{He–Hd,f}$ = 7.49]
Hf	7.52 [$^{3}J_{Hf–He}$ = 7.65] [$^{4}J_{Hf–Hd}$ = 1.54]	7.18 (d) [$^{3}J_{Hf–He}$ = 7.48] [$^{4}J_{Hf–Hd}$ = 1.61]	7.38 (d) [$^{3}J_{Hf–He}$ = 7.38]	7.23 (m)	7.25 (m)
Hg, g′	–	–	–	3.20 (m)	3.05 (m) and 3.15 (d, m)
Hh	–	–	–	1.82 (s)	3.55 (m)
Hh′	–	–	–	1.73 (m)	3.69 (m)
CH_2	–	4.45 (d) [$^{3}J_{HNCH}$ = 6.64]	4.75 (d) [$^{3}J_{P–H}$ = 12.96]	5.11 (d) [$^{3}J_{P–H}$ = 12.45]	5.05 (d) [$^{3}J_{P–H}$ = 12.94]
CH_3 ^{14}	2.60	2.49	2.68	2.41	2.42
CH_3 ^{15}	2.40	2.15	2.46	2.18	2.90
C1	164.27	154.8	157.3	155.7	156.5
C2	118.09	106.8	119.1	117.3	118.5
C3	157.72	149.4	149.7	146.8	147.4
C4	117.22	113.5	107.1 [$^{3}J_{P–C4}$ = 6.32]	112.0	112.9
C5	149.82	126.6	124.9 [$^{2}J_{P–C5}$ = 7.57]	128.0 [$^{2}J_{P–C5}$ = 6.30]	128.5
C6	157.07	1563.4	149.2 [$^{3}J_{P–C6}$ = 8.30]	151.7 [$^{3}J_{P–C6}$ = 8.90]	151.2 [$^{3}J_{P–C6}$ = 8.90]
C7	119.04	118.3	119.2	117.6 [$^{4}J_{P–C7}$ = 5.92]	117.9 [$^{4}J_{P–C7}$ = 6.44]
C8	133.34	129.4	126.8	127.0	127.2
C9	119.12	119.4	125.1	123.2	123.6
C10	133.52	131.0	129.7	128.1	128.5
C11	161.93	156.7	154.7	155.1	154.8 [$^{2}J_{P–C11}$ = 8.2]
C12, 12′	–	–	–	46.1 (d) [$^{2}J_{PNC12}$ = 15.4]	44.7 (d) [$^{2}J_{PNC12}$ = 12.4]
C13, 13′	–	–	–	26.4	67.1
C14	24.21	22.6	24.2	24.3	24.2
C15	20.83	20.9	21.4	20.9	21.4
CH_2	–	42.6	47.7	46.5	47.2

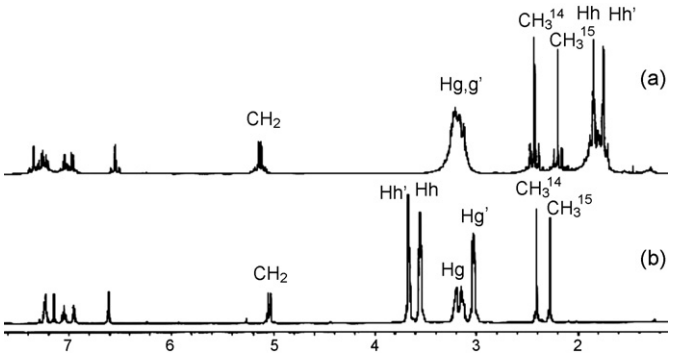

Fig. 2. ^{1}H NMR spectrum in δ 1–8 ppm for: (a) compound **4** and (b) compound **5**.

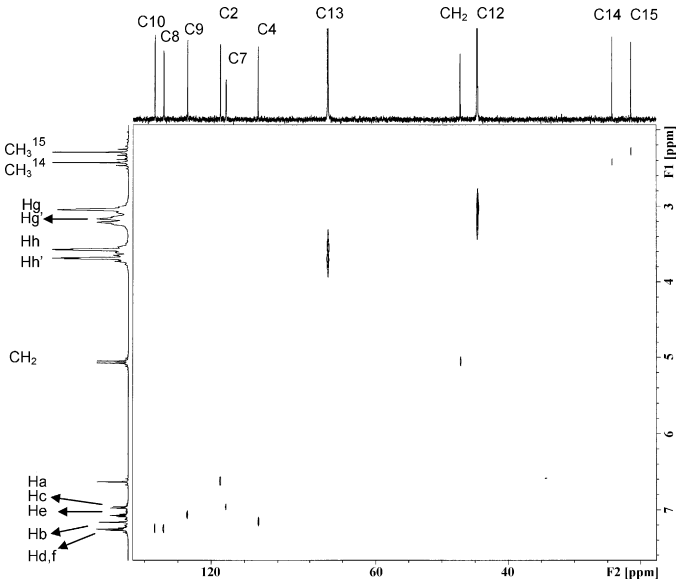

Fig. 4. HETCOR spectrum of **5**.

are distinguishable from each other and resonate at 3.20 ppm for **4**; 3.05 and 3.15 ppm for **5** and 1.82 and 1.73 ppm for **4**; 3.55 and 3.69 ppm for **5**. The Ar–CH_2–N– protons of (**3**–**5**) δ = 4.75, 5.11 and 5.05 ppm as doublets, in which those have three bond-coupling constants, ca. $^{3}J_{PH}$ = 12.78 Hz (Fig. 2).

All of the possible carbon peaks are observed from the ^{13}C NMR spectral data, as expected. The average four bond-coupling constant, $^{4}J_{PC}$, of Ar–CH_2–N is found 6.18 Hz. It is interesting that the two bond-coupling constants, $^{2}J_{PC}$, of C5 carbons of **3**–**5** are observed in the range of 6.30–7.57 Hz, which are smaller than those of the C6 carbons (Fig. 3 and Table 4).

Assignments of the protonated carbons were made by two-dimensional heteronuclear-correlated experiments (HETCOR, Fig. 4) using delay values which correspond to ^{1}J(C,H). As an example, only the HETCOR spectrum of **5** is depicted in Fig. 4. The peaks at δ = 118.5, 112.9, 117.9, 127.2, 123.6, 128.5, 44.7 and 67.1 ppm have been assigned them to C2, C4, C7, C8, C9, C10, C12 and C13 carbon atoms. In **5**, the absence of any contours at δ = 156.5, 147.4, 128.5, 151.2 ($^{2}J_{PNC}$ = 8.9 Hz) and 154.8 ($^{2}J_{PNC}$ = 8.2 Hz) ppm assign them to the C1, C3, C5, C6 and C11 carbon atoms, respectively. They belong to non-protonated atoms on the pyridine ring, C1, C3, C5 and on the phenyl ring carbons, respectively, all of which are unable to show any direct ^{1}H–^{13}C coupling interactions. C1 carbon atom adjacent to the more electronegative nitrogen atom of pyridine ring is shifted further downfield when compared to the neighboring and C5 carbon atoms. In addition, the carbon atom at para

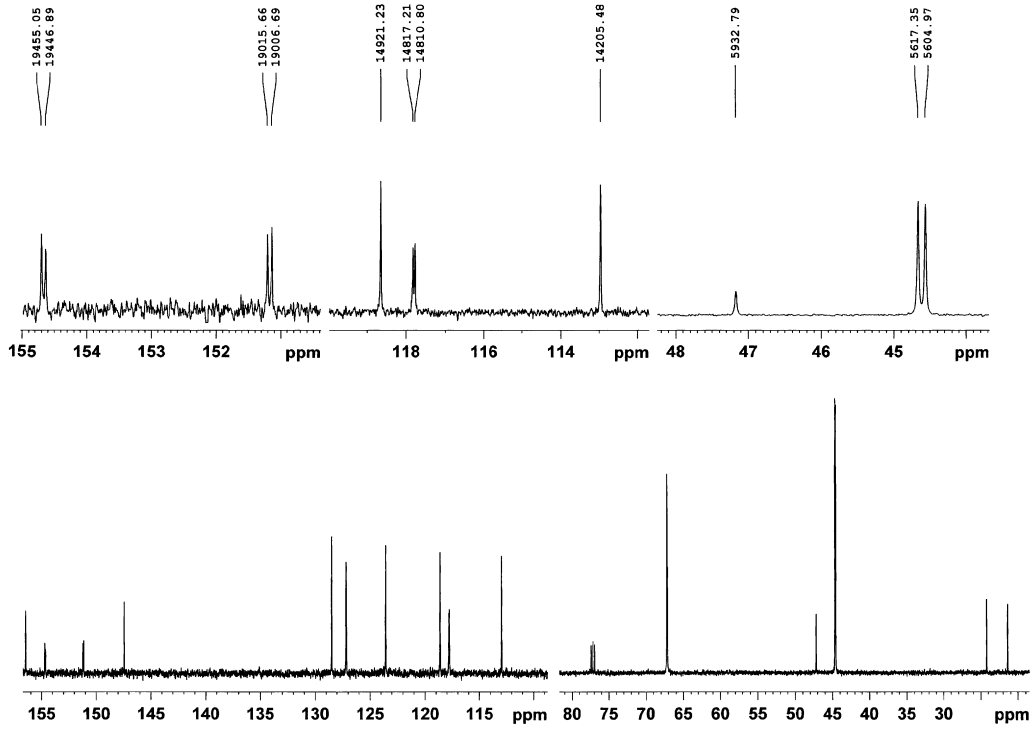

Fig. 3. ^{13}C NMR spectrum in 10–160 ppm for **5**.

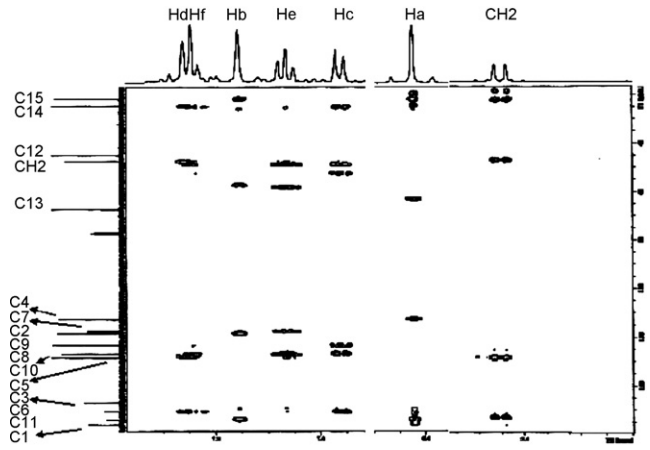

Fig. 5. HMBC correlations for **5**.

Table 5
2D ^{1}H–^{13}C HETCOR and HMBC correlations for **5**

Atom	HETCOR	HMBC [J(C,H)]			
	^{1}J	^{2}J	^{3}J	^{4}J	$^{intra}J$
Ha	C2	C1, C3	C14, C15	–	C13, 13′
Hb	C4	–	C15	–	C7, C11, C14
Hc	C7	C6, C8	C9, CH_2	–	C14
Hd	C8	–	C6	–	C14, CH_2
He	C9	C8, C10	C7	C6	C14
Hf	C10	–	C6	–	C14, CH_2
Hg, g′	C12	C13	–	–	$CH_3{}^{14}$
Hh, h′	C13	C12	–	–	–
CH_2	CH_2	C6	C5	C10	C14, C15
$CH_3{}^{14}$	C14	C1	–	–	C4, C7, C8, C9, C10
$CH_3{}^{15}$	C15	C3	C4, C2	–	C12

Intra: intramolecular interaction.

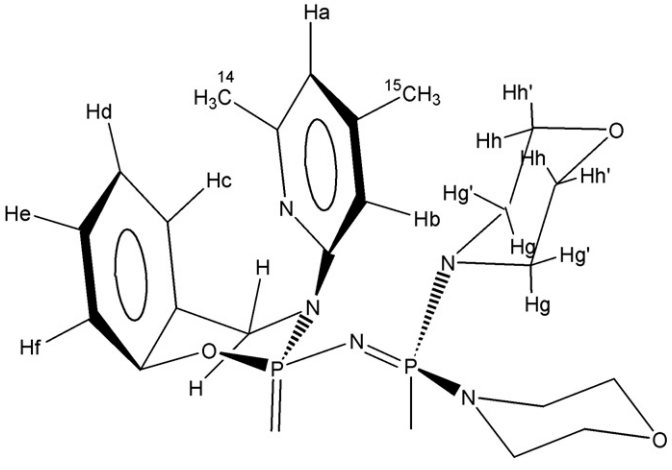

Fig. 6. The possible stereoisomer structure of compound **5** at ambient temperature in $CDCl_3$.

position to heteroatom, viz. C3 resonates at lower field value when compared to the meta positioned carbons, C2 and C4. However, the non-protonated carbon C5 is more shielded than C1 and C3 carbon atoms in the pyridine ring. On the other hand, the non-protonated carbons C1, C3, C5, C6 and C11 of compound (**5**) were also determined using delays in the two-dimensional HMBC experiment to emphasize the long range coupling, either ^{2}J(C,H) or ^{3}J(C,H) between the carbons and protons (Fig. 5 and Table 5). Consequently, according to the NMR results (HETCOR and HMBC) the probable conformation of compound **5** in $CDCl_3$ solution is depicted in Fig. 6, as an example.

Acknowledgements

The authors wish to acknowledge financial support of this work under grants Commission of Scientific Research Projects (grant no. 061037). We also thank Anadolu University and Medicinal Plants and Medicine Research Center of Anadolu University, Eskişehir, for allowing us to use the NMR facility.

References

[1] C.W. Allen, in: I. Haiduc, D.B. Sowerby (Eds.), The Chemistry of Inorganic Homo- and Hetero-cycles, vol. 2, Academic Press, London, 1987 (Chapter 20).
[2] R.H. Neilson, W.P. Neilson, Chem. Rev. 88 (1988) 541.
[3] H.R. Allcock, Chem. Eng. News 18 (1985) 22.
[4] V. Chandrasekhar, K.R. Justin Thomas, Struct. Bond. 81 (1993) 41.
[5] C.W. Allen, in: I. Haiduc, D.B. Sowerby (Eds.), The Chemistry of İnorganic Homo and Heterocycles, vol. 2, Academic Press, London, 1989, p. 133.
[6] J.E. Mark, H.R. Allcock, R. West, Inorganic Polymers, Prentice-Hall, Englewood Cliffs, NJ, 1992.
[7] P.M. Blonsky, D.F. Shriver, P. Austin, H.R. Allcock, Solid State Ionics 18 (1986) 258.
[8] D.F. Shriver, G.C. Ferrington, Chem. Eng. News (1985) 45.
[9] H.R. Allcock, R. Eric, L. Didier, A. Mireille, C. Jean-Pierre, Macromolecules 29 (1996) 1951.
[10] R.A. Bartsch, E.K. Lee, S. Chun, N. Elkarim, K. Brandt, I. Parwolik-Czomperlik, M. Siwy, D. Lach, J. Silberring, J. Chem. Soc., Perkin Trans. 2 (2002) 442.
[11] H. Beak, Y. Cho, C.O. Lee, Y.S. Shon, Anti-cancer Drugs 11 (2000) 715.
[12] V. Konar, Ö. Yılmaz, A.İ. Öztürk, S. Kırbağ, M. Arslan, Bioorg. Chem. 28 (2000) 214.
[13] K. Brandt, R. Kruszynski, T.J. Bartczak, I. Parwolik-Czomperlik, Inorg. Chim. Acta 322 (2001) 138.
[14] L.S. Nair, D. Lee, C.T. Laurencin, Handbook of Biodegradable Polymeric Materials and their Applications, vol. 1, 2006, p. 277.
[15] Bruker program 1D WIN-NMR (release 6.0) and 2D WIN-NMR (release 6.1).
[16] H. Dal, S. Safran, Y. Süzen, T. Hökelek, Z. Kılıç, J. Mol. Struct. 753 (2005) 89.
[17] N. Çaylak, T. Hökelek, O. Büyükgüngör, H. Dal, Y. Süzen, Z. Kılıç, Acta Cryst. E61 (2005) 1557.
[18] R.A. Shaw, Phosphorus Silicon 28 (1986) 99.
[19] S. Bilge, B. Özgüç, Ş. Demiriz, H. İşler, M. Hayvalı, Z. Kılıç, T. Hökelek, J. Mol. Struct. 748 (2005) 101.